Preliminary analysis of the March 9, 1997 solar eclipse observations

T. Pintér[1], M. Lorenc[1], B. Lukáč[1], M. Minarovjech[2], D. Očenáš[3], M. Rybanský[2] and J. Sýkora[2]

[1] *Slovak Central Observatory, 94701 Hurbanovo, The Slovak Republic*

[2] *Astronomical Institute of the Slovak Academy of Sciences 059 60 Tatranská Lomnica, The Slovak Republic*

[3] *Observatory, 97590 Banská Bystrica, The Slovak Republic*

Received: July 16, 1997

Abstract. Observations of the solar corona carried out during the March 9, 1997 total solar eclipse are described, and the goals of experiments are mentioned. The photometry of the white-light images shows the form of the solar corona typical for the near-minimum phase of solar cycles, i.e. considerably flattened towards the solar equator and abundant in polar coronal rays. We managed to add current observations of the emission corona and prominences, made with the coronagraph of the Lomnický Štít Observatory to the eclipse data. Profiles of the 'green' and 'red' emission corona brightness at a standard height of 40 sec of arc above the Sun's limb are presented here, while full analysis of a the large number of extra-eclipse measurements will take more time.

Key words: solar eclipse – solar corona – photometry – flash spectrum – extra-eclipse emission corona brightness

1. Introduction

Eclipse observations of the solar corona are certainly still justified and valuable. They provide an excellent possibility of identifying different coronal structures ranging in distance from near the limb to several Sun's radii. Moreover, precise photometry and, consequently, a detailed study of their physical properties is feasible. As regards the field of view and spatial resolution, the eclipse images of the solar corona are unsurpassed by any other imaging coronal observing device used outside eclipses.

The individual authors of the present paper have observed a number of solar eclipses, beginning with the June 30, 1973 eclipse. The past results include, first of all, determination of the absolute coronal intensities and electron densities for discrete coronal structures and in dependence on the position angle (Rušin and Rybanský, 1975; 1985a). Integral coronal brightness and flattening of the

corona were described as a function of the solar cycle phase (Rušin and Rybanský, 1983a; 1985b). The solar activity on the disk and its effects in the variety of the eclipse coronal structures were also studied (e.g. Rušin and Rybanský, 1976; 1979; 1983b). The volume emission measure of the inner corona arch systems has been estimated by analysing the images of the green-line FeXIV 530.3 nm corona (Badalyan, Livshits and Sýkora, 1984). Distributions of brightness and polarization of the white-light corona and its large-scale structure in the period of the solar-cycle maximum were studied under the assumption of Thomson scattering (Badalyan, Livshits and Sýkora, 1993). The behaviour and general properties of white-light polarization in helmet-streamers and coronal holes were investigated using the data of three eclipses (Badalyan, Livshits and Sýkora, 1997). The analysis of polarization of the green-line corona in the July 11, 1991 eclipse revealed a physically meaningful anticorrelation between the degree of polarization and the green-line corona brightness. It seems that this finding contains information about the role of electron collisions in the excitation of the green coronal line and about certain physical properties of the coronal magnetic field (Badalyan and Sýkora, 1977). Structures, global coronal forms and flattenings of several eclipse coronae were investigated in relation to the calculated heliospheric magnetic field topology. Doubts were cast on the generally accepted Ludendorff's definition of coronal flattening and on the historically derived dependence of the coronal flattening index with the solar-cycle phase (Sýkora and Ambrož, 1995; 1997; Sýkora, Pintér and Ambrož, 1995).

The present paper describes the March 9, 1997 eclipse corona structures and presents the traditional discussion of the coronal flattening and the results of the relative photometry of this corona. The latter are compared and discussed in connection with the absolute photometry of emission coronal lines, performed by the coronagraph of the Lomnický Štít Observatory on and around the eclipse day. Newly included experiment of recording the flash spectra is described.

2. Geometry of the eclipse

The six-man expedition of the Slovak Central Observatory, Hurbanovo (Slovak Republic) was dispatched to the path of totality near the town of Pervomaiskii (Eastern Siberia, Russia). The local coordinates and eclipse parameters are given in Table 1, while the geometry of this eclipse is shown in Fig. 1. The quantity $+\alpha$ denotes the direction in which the right ascension increases and, in fact, this line represents the declination parallel passing through the Sun's centre at the time of totality.

3. Observations

The expedition successfully performed planned experiments and the corresponding measurements were completed by the extra-eclipse observations of the solar

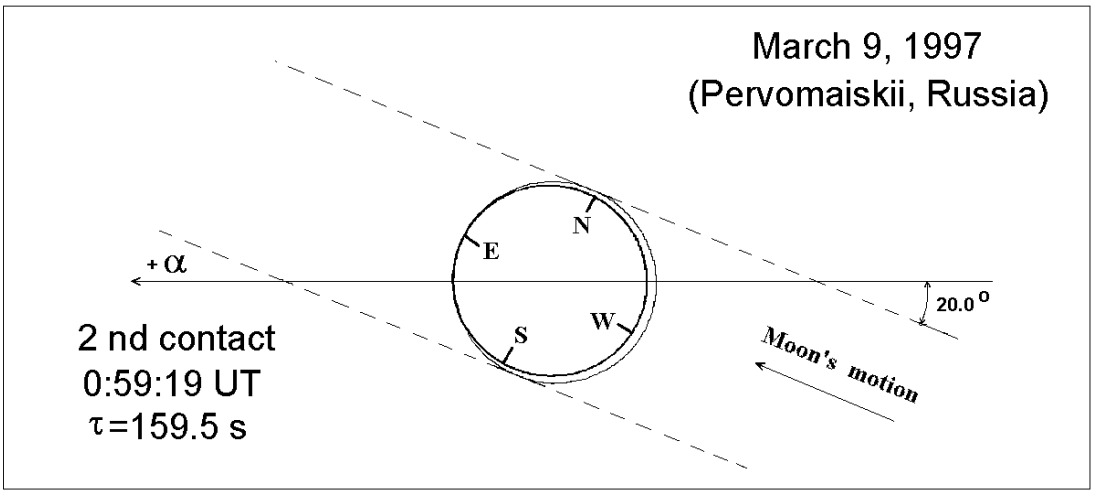

Figure 1. Geometry of the March 9, 1997 total solar eclipse at Pervomaiskii (Russia).

Table 1. Parameters of the March 9, 1997 eclipse at Pervomaiskii (Siberia, Russia).

Geographic longitude	115° 39' 44" E
Geographic latitude	51° 36' 44" N
Altitude	about 750 m
2nd contact (observed)	$00^h\ 59^m\ 19^s$ UT
3rd contact (observed)	$01^h\ 01^m\ 59^s$ UT
Heliographic position angle of the 2nd contact	95.7°
Umbral duration	$2^m\ 40^s$
Eclipse magnitude	1.020
Solar corona covered by the Moon at the middle of totality	up to 40"
Zenith distance of the Sun	73°
Path width	366 km
Distance of the locality from the central line of the eclipse	About 6 km to the south
Position of solar rotation axis	P = + 23.4°

corona.

(1) Structure and photometry of the white-light corona

An 80-millimetre f/15 telescope, equipped with a commercial Pentacon-Six camera, was used to photograph the white-light corona. Four images with exposures of 1/4 sec, 1/15 sec, 1/60 sec and 1/1000 sec were taken on KODAK T MAX 400 60-millimetre roll-film. In fact, it was planned to take more images but, unfortunately, the ambient temperature of $-25°$C caused the camera shutter to malfunction. To obtain relative intensities, photometric scales were recorded by photographying the sunset sky at zenith with the same exposures. One of the purposes of the experiment was to identify different coronal structures and to derive the distribution of coronal brightness all around the solar limb up to a distance of about r = 3.0 $R_\odot$. T.P. was the observer of this experiment. In addition, eighteen exposures from 1/1000 sec to 7 sec were made on KODAK 200 ASA Color film using an f = 500 mm tele-lens. All the images are of very good quality. They will be processed by overlapping-images technique to increase the contrast of the structures. Special emphasis will be given to clear identification of the system of coronal rays in both solar polar regions. This part of experiment was performed by D.O.

(2) Flash spectrum

Shortly after the second contact, the spectrum of chromosphere (the region of 480–660 nm) was photographed by using a reflecting 80x80 mm grating, 651 grooves/mm, located in front of the lens d = 75 mm, f/4. A KODAK T MAX 400 film was also used in this case. In all, two spectra were recorded at exposures of 1/30 sec and 1/15 sec. The relative photometry of the hydrogen and helium lines should give a more precise estimate of the helium abundance in the chromosphere. The observations were conducted by B.L.

(3) Coronagraphic observations

Apart from the real eclipse experiments, extended extra-eclipse observations were carried out by the staff of the Lomnický Štít coronal observatory. Twelve hours prior to the eclipse and five hours after the eclipse, patrol observations of prominences and photometry of the 530.3 nm and 637.5 nm emission coronal lines were realized. Special measurements of the FeXI - 789.2 nm and FeXIII - 1075 nm and 1080 nm emission line intensities were repeated several times in the chosen region around position angle 300°. M.M. and M.R. performed the measurements.

4. Preliminary results

At present, we are only able to provide partial results of the eclipse experiments. As for the patrol extra-eclipse observations, we present and discuss here the distribution of prominences around the solar disk, and we compare the intensities of the emission lines at different position angles with the white-light corona brightness and with the presence of separated eclipse coronal structures

on the solar limb. The analysis of the more detailed coronagraphic data will be published separately.

4.1. Structure and photometry of the (K+F) corona

The global structure of the March 9, 1997 solar corona is displayed in Fig. 2. To a large extent, the lines drawn on our coronal sketch, in fact, represent the structure of the large-scale coronal magnetic field lines of force, and they also indicate some of their fingers extending into the heliosphere (Sýkora and Ambrož, 1997). This sketch was obtained by considering the photographic and

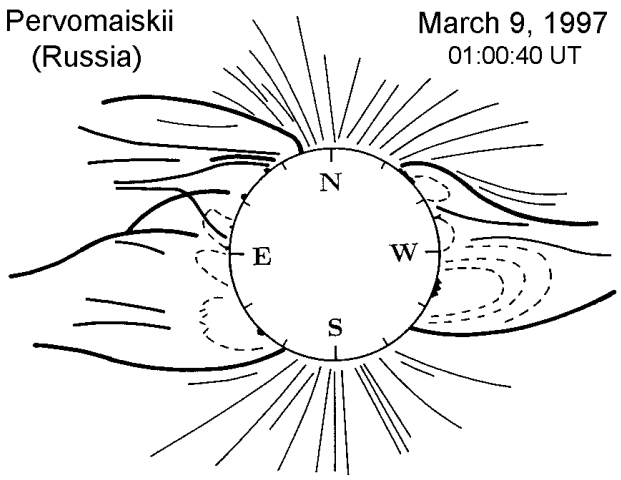

Figure 2. Drawing of the March 9, 1997 coronal structures.

computer processing of the same white-light corona image. A well-known photographic method of enhancing the contrast of the structures consists in a combination of the negative and positive of the same original image, and their mutual rotating through a small angle of the order of one arc degree. The computer processing of the digitized image included successive using of two-dimensional fast Fourier transformation, digital filtration and application of the numerical unsharp masking method. This procedure allowed the adequate image resolution of the different coronal structures to be obtained. An example of the computer-processed image is shown in Fig. 3. We are convinced that applying and synthesizing the mentioned two techniques are capable of yielding more realistic drawings of the coronal structures than can be derived by processing eclipse corona images taken through commonly used neutral radial density filters. This is because we are working with the original 'undeformed' coronal images, whereas if the neutral density filter is used, the resulting coronal images are 'deformed' in brightness and the 'original' image of the solar corona can never be really restored.

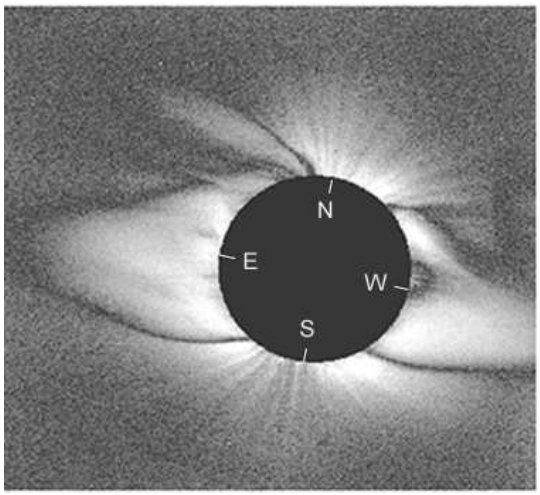

Figure 3. Computer-processed structure of the eclipse corona.

It is evident that the March 9, 1997 corona is still perfectly of the 'minimum type', typical for the periods near to solar-cycle minima. Moreover, it is interesting that a clearly bipolar corona, with well-developed polar rays and characterictic by the heliographic equator being more or less identical with the solar magnetic equator, has now been persisting for at least three years. We remind the reader that the coronal forms of the 1994 and 1995 solar eclipses (e.g. Sýkora et al. 1997) are very similar to the form of the 1977 corona. Thus, during about three years of the solar cycle No. 22 minimum the changes of coronal toplogy were negligible. Cliver (1993) mentioned a similar situation aloso occured in case of cycle No. 20, whereas the bipolar character of the corona persisted for a considerably shorter period of time during the minima of odd cycles Nos 19 and 21. This seems to be connected with the different morphological properties of the even and odd 11-year solar cycles creating, in fact, the 22-year solar magnetic cycle (Cliver, Boriakoff and Bounar, 1996, Storini and Sýkora, 1997).

The level of solar activity was even somewhat lower in March 1997 than it was 2–3 years ago when the 'minimum type' eclipses of November 3, 1994 and October 24, 1995 took place. The more is the 1997 corona also characterized by extended regions of fine and pronounced polar coronal rays at the both solar poles (covering about 60° of position angles (p.a.) at the northern pole and about 70° at the southern). At the same time, these sets of the polar rays indicate the presence of polar coronal holes, clearly recognizable, for example, on the YOHKOH SXR eclipse day image. The polar coronal rays are radially oriented directly at the poles, and increasigly inclined towards the equator as they proceed from the poles to lower latitudes. The boundaries between the polar-ray regions and the regions of the more active low-latitude corona are very distinct

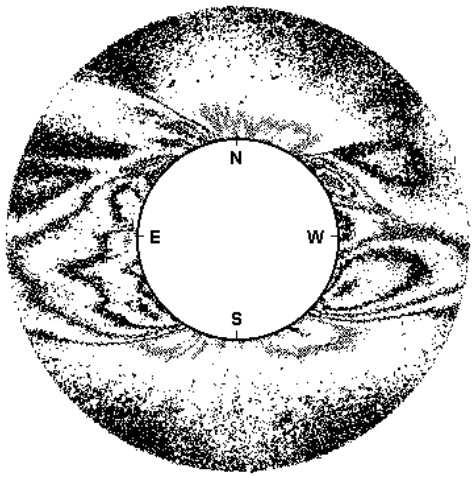

Figure 4. Computer-processed isodensities of the eclipse corona.

and unusually sharp. This is seen, for example, in the computer-processed Figs 3 and 4. Although these figures should be considered as highly qualitative, they nevertheless provide valuable information about the distribution of brightness within the different coronal structures described below.

The north pole coronal hole is not quite symmetrically extended around the pole, being more shifted to the west. Therefore, the east limb 'active' corona already starts at p.a. of about 15° with an enhanced, approximately 13° broad inclined elongated feature, which can hardly be considered a coronal streamer. At its anchorage to the solar limb, this feature is clearly separated from the neighbouring structure representing a well-developed coronal streamer. From the projection of this streamer on to the plane of the sky (the plane of the image) the following parameters can be deduced: its base on the limb covers about 40° (from 30° to about 70° of the p.a.), the neutral point of the streamer's dome structure is located at a height of only r = 1.35 $R_\odot$ (the solar surface being r = 1.0 $R_\odot$) and the streamer's neutral current sheet is highly inclined towards the radial direction by about 30°, clearly twisting sa it recedes from the Sun. Considering all above parameters, the streamer seems to be anchored to the solar surface rather far from the limb. Without any distinct separation from the previous streamer, another huge streamer-like structure is seen at the east limb, displaying a sharp dome boundary at the p.a. of 150°. We are of opinion that, due to the evident differences in the inner brightness and structuring, this feature can hardly be considered to be one compact coronal streamer. Apart from this, clear condensations in coronal brightness (c.f. activity) are seen close to the limb in this streamer-like region. It is more probable that this structure, in fact, represents several somewhat minor streamers projected one on to another.

The west limb corona is simpler in its structuredness. In principle, two

streamers are seen only, clearly separated by a deep decrease of the coronal brightness centred at the p.a. 270°–290°. The large streamer in the SW quadrant (p.a. 220°–270°) is clasically developed, with evident loop structures and a prominence within the dome, the neutral point being at the usually accepted coronal source surface r = 2.5 $R_\odot$. A smaller but brighter streamer in the NW quadrant (p.a. 290°–320°) is practically a mirror-streamer of the first one described in this Section. The inclination of the neutral current sheet to the radial direction is also high (about 30°), the neutral point being located also rather low – at about r = 1.45 $R_\odot$. Therefore, the real position of this streamer is again, most likely, well outside the solar limb.

Table 2. Relative intensities for the isophotes listed in Fig. 5.

Number of isophote	Relative intensity
1	4.519
2	3.896
3	3.584
4	3.270
5	3.033

Figs 2–4, of course, provide the possibility of good identification and qualitative description of the different coronal structures. However, it is understandable that no drawing of the coronal structures has to correspond to the true quantitative distribution of the coronal brightness and reflect the real shape (form) of the global solar corona. On the other hand, the application of more quantitative methods of image analysis usually cannot satisfactorily fulfil demands on a more precise identification of the structures. Both the approches are, in fact, complementary. In Fig. 5 we present the result of the relative photometry of the (K+F)-corona. The white-light coronal image was scanned with a resolution of 0.5 arc sec (the whole image represents measurements in 765x510 pxs). Five isophotes are demonstrated, their relative intensities being given in Table 2. The relative intensity at any point of the solar corona can be estimated, in the first approximation, by interpolation.

No structural details of the solar corona are seen in Fig. 5. This figure, for example, does not display so pronounced decrease of coronal brightness at the poles as indicated by Figs 2–4. On the other hand, to quantify the flattening of the solar corona the isophotes are indispensible. Traditionally, Ludendorff's definition is used to calculate the coronal flattening. Let d_1 be the average of the equatorial diameter of the coronal isophote and of the two diameters that make an angle of 22.5° with the equator; let d_2 be the similar average diameter of the same coronal isophote at the polar axis and at the two diameters that make an angle of 22.5° with the polar axis. Ludendorff (1928) then defines the

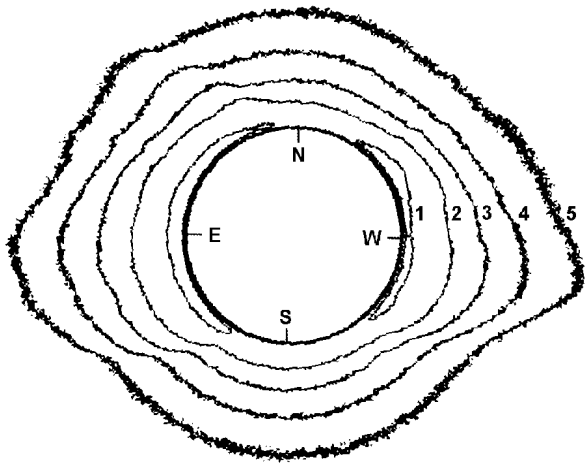

Figure 5. Isophotes of relative intensities. If logarithm of intensity 4.7 ($I = 5 \times 10^{-6} I_0$) is attributed to the brightest region of the eclipse solar corona (situated around p.a. 98°) then the log(I) for different isophotes are as given in Table 2.

'flattening of the corona' by the parameter

$$\varepsilon = \frac{d_1}{d_2} - 1. \tag{1}$$

Using our data, the flattening of the March 9, 1997 eclipse corona is $\varepsilon = +0.202 \pm 0.007$ at r = 2.0 $R_\odot$. Such a high value of the coronal flattening is typical for periods of the solar-cycle minima. In agreement with the known dependence of the coronal flattening on the phase of the solar cycle, this value is even higher than found (Sýkora et al., 1997) for the 1994 and 1995 eclipses of the present cycle minimum ($\varepsilon = +0.125$ and $\varepsilon = +0.133$, respectively).

4.2. Flash spectrum

The flash spectrum of the chromosphere was recorded at the point of the 2nd eclipse contact. The usual procedure was applied to determine the wavelengths of the spectral emission lines. Lines H_β, NaI (D_1 and D_2) and MgI (b_1, b_2, b_3) were taken as reference. The relative intensities were estimated using calibration curve created from an image of the 9-step scale photographed immediately after the eclipse on the same film strip. Preliminary results are given in Table 3.

The first column gives the estimated wavelengths with an accuracy of 0.1 nm. The relative intensities given in the second column are referred to the intensity of the H_β line which was taken to be 100. Tentative identification of the corresponding ions together with their laboratory wavelengths are shown in the last two columns, respectively.

Table 3. List of the recorded flash spectrum lines.

λ [nm]	Intensity	Element (Ion)	Laboratory λ [nm]
486.1	100	HI	486.100
491.5	15	FeII	492.392
501.2	30	FeI	501.843
516.3	48	MgI	516.455
517.3	47	MgI	516.767
518.3	11	MgI	518.431
530.3	9	FeXIV	530.276
587.6	104	HeI	587.577
590.0	27	NaI	589.244
637.4	7	FeX	637.455

Notice that among the recorded lines are also the 'green' FeXIV 530.3 nm and 'red' FeX 637.4 coronal emission lines. The estimated relative intensities of these lines can be compared with the extra-eclipse measurement of these lines (see Subsection 3) performed on the absolute photometric scale. Taking this comparison into account, a rough estimate of the absolute intensities of all the identified flash spectrum lines can be made.

4.3. Coronagraphic observations

Prominences observed during the patrol service at the Lomnický Štít Observatory on March 8 and 9, 1997, early in the morning (06:00 UT), are listed in Table 4. The first column refers to the date of observation. The heliographic longitude and latitude of the recorded prominences are given in the next two columns, respectively. The extent of prominences (in arc degrees on the solar limb) can be found in the fourth column, while the fifth column gives the heights of the prominences in arc seconds. The estimations of the prominence brightness on the 3-step scale and area occupied by the prominence in arbitrary units are presented in the last two columns of this Table.

It is seen that the prominence activity was somewhat higher on March 9 than on the preceding day. Generally, the prominences were relatively small and inactive. Besides the patrol service, other observations of prominences on March 9 were made some 12 hours after the eclipse time. These are plotted in Fig. 2 as the small black areas around the solar limb. The comparison of this set of promineces with that listed in Table 4 indicates only small changes in their position and area over about 7 hours.

The intensities (expressed in so-called absolute coronal units) of the 'green' and 'red' coronal lines around the solar disk (position angles vary from 0° to 360°) are presented in Fig. 6 for the eclipse day and the preceding day. These data are, as usual, related to the very low corona (40 arc sec above the solar

Table 4. List of prominences observed by coronagraph.

Date	Longitude	Latitude	Extent	Height	Brightness	Area
97 03 08	186.9	+51.4 E	1	20	2	20
97 03 08	182.3	+30.7 E	3	50	2	80
97 03 08	0.8	-20.8 W	6	40	2	150
97 03 08	355.1	+21.8 W	2	20	2	50
97 03 08	350.8	+45.5 W	3	20	1	50
97 03 09	171.7	+42.6 E	3	30	1	60
97 03 09	170.2	+35.7 E	3	40	2	60
97 03 09	167.3	+17.9 E	2	40	1	50
97 03 09	165.8	+6.0 E	3	40	1	50
97 03 09	158.1	-43.6 E	3	30	2	60
97 03 09	347.3	-17.9 W	5	40	2	120
97 03 09	342.9	+15.9 W	4	50	1	130
97 03 09	337.8	+44.5 W	15	30	3	330

limb) and in no case can they be interpreted in terms of the height of different coronal structures. On the other hand, it is well-known that the intensity of the 'green' emission line is directly proportional to the density and temperature of the medium where this line originates. Thus, the intensity of the 'green' line is a very good indicator of general coronal activity ahd rather high correlation between the enhanced green-line intensity regions and the enhanced brightness of the white-light corona structures usually follows.

The following conclusions can be drawn from Fig. 6:

– The general level of the green-line intensity on the eclipse day (namely at the W limb) is slightly increased in comparison with its usual level at this phase of the solar cycle (deep minimum).

– The differences between the 8 and 9 March intensities are small, sometimes they can be more dramatic in the course of a single day.

– The polar coronal holes are identified distinctly by neglible green-line intensity.

– A deep decrease of the green-line intensity at p.a. 280°–290° corresponds very well with the above-mentioned decrease of white-light brightness between the two W-limb streamers.

– The comparison of the brightness and structures seen in the white-light photograph of the eclipse corona (which we are not able to publish here in satisfactory quality) with the distribution of the green-line corona intensity confirms better than average correlation of both the quantities.

– The intensity of the red-line corona is more uniformly distributed and, as usual and understandably, it does not reflect the structuredness of the white-light corona well. A general increase of the red-line intensity of about ten absolute coronal units from 8 to 9 March can be, to a large extent, due to different 'sky

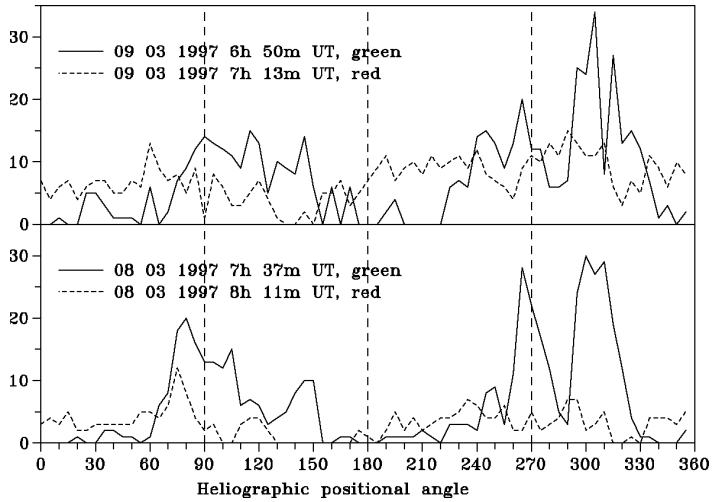

Figure 6. Absolute intensities of the 'green' and 'red' coronal emission lines around the Sun on the eclipse and the preceedings days.

conditions' on both days.

Acknowledgements. The authors gretly appreciate the support of the Slovak Ministry of Culture, the financial contributions of a number of private sponsors in respect of the eclipse expedition, and Grants Nos 2004/95 and 2007/95 of the Slovak Grant Agency for Science (VEGA) in support of this research.

References

Badalyan, O.G., Livshits, M.A., Sýkora, J.: 1984, *Solar Phys.* **93**, 143.
Badalyan, O.G., Livshits, M.A., Sýkora, J.: 1993, *Solar Phys.* **145**, 279.
Badalyan, O.G., Livshits, M.A., Sýkora, J.: 1997, *Solar Phys.* **173**, 67.
Badalyan, O.G., Sýkora, J.: 1997, *Astron. Astrophys.* **319**, 664.
Cliver, E.W.: 1993, *J. Geophys. Res.* **98**, 17435.
Cliver, E.W., Boriakoff, v., Bounar, K.H.: 1996, *J. Geophys. Res.* **101**, 27091.
Ludendorff, H.: 1928, *Sitzber. Preuss. Akad. Wiss.* **16**, 185.
Rušin, V., Rybanský, M.: 1975, *Bull. Astron. Inst. Czechosl.* **26**, 206.
Rušin, V., Rybanský, M.: 1976, *Bull. Astron. Inst. Czechosl.* **27**, 279.
Rušin, V., Rybanský, M.: 1979, *Bull. Astron. Inst. Czechosl.* **26**, 206.
Rušin, V., Rybanský, M.: 1983a, *Bull. Astron. Inst. Czechosl.* **34**, 257.
Rušin, V., Rybanský, M.: 1983b, *Bull. Astron. Inst. Czechosl.* **34**, 265.
Rušin, V., Rybanský, M.: 1985a, *Bull. Astron. Inst. Czechosl.* **36**, 74.
Rušin, V., Rybanský, M.: 1985b, *Bull. Astron. Inst. Czechosl.* **36**, 77.
Storini, M., Sýkora, J.: 1997, *Solar Phys.* , in press.
Sýkora, J., Ambrož, P.: 1995, in *24th International Cosmic Ray Conference* **4**, ed.: N. Iucci, Roma, 509.

Sýkora, J., Pintér, T., Ambrož, P.: 1995, *Revista de la Academia Nacional de Ciencias de Bolivia* **No. 69**, 23.

Sýkora, J., Ambrož, P.: 1997, in 'Theoretical and Observational Problems Related to Solar Eclipses', eds.: Z. Mouradian and M. Stavinschi, Kluwer Academic Publishers, Dordrecht, *NATO ASI Series C: Mathematical and Physical Sciences*, **494**, 111.

Sýkora, J., Ambrož, P.,Kotrč, P., Minarovjech, M., Pintér, T., Rybák, J., Rybanský, M.: 1997, in 'Theoretical and Observational Problems Related to Solar Eclipses (Poster Papers)', ed.: G. Maris, Bucharest, *Roumanian Astron. J.*, in press.